NeuroImage 217 (2020) 116898

Contents lists available at ScienceDirect

NeuroImage

journal homepage: www.elsevier.com/locate/neuroimage

Distinct fMRI patterns colocalized in the cingulate cortex underlie the after-effects of cognitive control on pain

Nicolas Silvestrini [a,b,*], Jen-I Chen [b], Mathieu Piché [c], Mathieu Roy [d], Etienne Vachon-Presseau [e,f,g], Choong-Wan Woo [h,i], Tor D. Wager [j,k], Pierre Rainville [b,l,m]

[a] Geneva Motivation Lab, Faculty of Psychology and Educational Sciences, University of Geneva, Geneva, Switzerland
[b] Research Center of the Institut Universitaire de Gériatrie de Montréal, Université de Montréal, Montréal, Canada
[c] Département de Chiropratique, Université Du Québec à Trois-Rivières, Trois-Rivières, Canada
[d] Department of Psychology, McGill University, Montréal, Canada
[e] Faculty of Dentistry, McGill University, Montréal, Canada
[f] Department of Anesthesia, McGill University, Montréal, Canada
[g] Alan Edwards Centre for Research on Pain (AECRP), McGill University, Montréal, Canada
[h] Center for Neuroscience Imaging Research, Institute for Basic Science, Suwon, Republic of Korea
[i] Department of Biomedical Engineering, Sungkyunkwan University, Suwon, Republic of Korea
[j] Department of Psychology and Neuroscience, University of Colorado, Boulder, CO, USA
[k] Institute of Cognitive Science, University of Colorado, Boulder, CO, USA
[l] Groupe de recherche sur le système nerveux Central, Université de Montréal, Montréal, Canada
[m] Department of Stomatology, Université de Montréal, Montréal, Canada

A B S T R A C T

Demanding tasks can influence following behaviors but the underlying mechanisms remain largely unclear. In the present functional magnetic resonance imaging (fMRI) study, we used multivariate pattern analyses (MVPA) to compare patterns of brain activity associated with pain in response to noxious stimuli administered *after* a task requiring cognitive control (Stroop) and evaluate their functional interaction based on a mediation analysis model. We found that performing a difficult cognitive task leads to subsequent increases in pain and pain-related multivariate responses across the brain and within the anterior mid-cingulate cortex (aMCC). Moreover, an aMCC pattern predictive of task performance was further reactivated during pain and predicted ensuing increases in pain-related brain responses. This suggests functional interactions between distinct but partly co-localized neural networks underlying executive control and pain. These findings offer a new perspective on the functional role of the cingulate cortex in pain and cognition and provide a promising framework to investigate dynamical interactions between partly overlapping brain networks.

1. Introduction

The interactions between pain and cognitive processes are strong but complex. Whereas analgesia during a distracting task is well documented (Buhle and Wager, 2010; Eccleston and Crombez, 1999; Legrain et al., 2009), it remains largely unclear how cognitively demanding tasks impact subsequent pain. Given that coping with difficult cognitive tasks is obviously frequent in daily life, it is crucial to improve our understanding of the influence of such cognitive exertion on clinically and socially important phenomena such as pain.

Numerous evidence suggests that performing a difficult task leads to impaired performance in following demanding behaviors (Hagger et al., 2010)—although this effect was also recently challenged (Hagger and Chatzisarantis, 2016). The strength model of self-control (Baumeister et al., 2018, 2007, 1998) proposed an early explanation of this effect, postulating a limited and domain-general self-regulatory resource that becomes depleted after a demanding task leading to impaired subsequent regulatory mechanisms (the so-called ego depletion effect). However, since then, other authors proposed alternative models and the underlying mechanisms are still highly debated (Inzlicht and Schmeichel, 2012; Kool and Botvinick, 2014; Kurzban et al., 2013; Wright and Mlynski, 2019). Previous research revealed reduced tolerance (Vohs et al., 2008) and increased pain responses (Silvestrini and Rainville, 2013) to noxious stimuli administered following the performance of demanding tasks. Therefore, these findings are in line with previous evidence showing impaired regulatory performance after demanding tasks. However,

* Corresponding author. Faculty of Psychology and Educational Sciences, Section of Psychology, University of Geneva, Boulevard du Pont-d'Arve 40, CH-1211 Geneva 4, Switzerland.
E-mail address: nicolas.silvestrini@unige.ch (N. Silvestrini).

https://doi.org/10.1016/j.neuroimage.2020.116898
Received 18 July 2019; Received in revised form 13 February 2020; Accepted 29 April 2020
Available online 4 May 2020

evidence is scarce and insights into neural underpinnings are lacking regarding pain.

Neuroimaging studies found that top-down regulation by prefrontal regions associated with cognitive control, mainly the anterior cingulate, the dorsolateral, and the ventrolateral prefrontal cortices, plays a central role in the impact of a demanding task on subsequent behavior (Inzlicht et al., 2016; Ochsner and Gross, 2005; Wagner et al., 2013; Wagner and Heatherton, 2012). However, these studies did not specifically investigate pain. Given the importance of cognitive processes in the experience of pain, further studies investigating underlying brain mechanisms are required.

In the present functional magnetic resonance imaging (fMRI) study, we used multivariate pattern analyses (MVPA) (Haxby et al., 2001; Wager et al., 2013; Woo et al., 2017) to determine whether pain and cognitive control engage distinct patterns of brain activity and, if so, how the processes reflected in these brain patterns interact. We administered noxious electrical stimulation following blocks of a cognitively demanding task (counting Stroop task, see method) compared to a control task involving low cognitive demand. We predicted stronger pain and pain-related brain responses after the task involving higher cognitive demand. We analyzed brain data using the Neurologic Pain Signature (NPS), a distributed pattern of fMRI activity previously shown to be sensitive and specific to nociceptive pain (Wager et al., 2013), and a fMRI pattern developed to discriminate between the high and low cognitive demand. Next, we focused on the anterior mid-cingulate cortex (aMCC) given its fundamental role in both pain and cognitive control (Davis et al., 1997; Shackman et al., 2011) and recent debates about its functional specificity (Critchley, 2004; Lieberman and Eisenberger, 2015; Shenhav et al., 2016; Wager et al., 2016). Previous research associated the anterior cingulate cortex (ACC) with affective processes and the mid-cingulate cortex (MCC; or posterior sector of the dorsal ACC) with cognitive function (Bush et al., 2000). However, in contrast to this anatomo-functional segregationist model, recent evidence supports the view that the anterior subdivision of the MCC (aMCC) implements a domain-general process common to pain, cognitive control, and negative affect (see Shackman et al., 2011, for a review). Therefore, drawing on this perspective, we investigated multivariate patterns within the aMCC developed to discriminate the experimental conditions during pain and cognitive control, and the relationship between these patterns using a mediation analysis.

2. Materials and methods

2.1. Participants

Twenty-four healthy volunteers participated in the study (16 females and 8 males; 22 right handed and 2 left handed; mean age 23 years; range 18–32). All participants were already familiarized with the painful stimulations, the pain rating scales, the nociceptive flexion reflex (NFR) threshold determination, and the task in the context of a previous experiment in the lab (Silvestrini and Rainville, 2013). The present fMRI study was conducted two months after this previous experiment. All participants provided signed informed consent and received a compensation of C$50 for their time and commitment to the study. All experimental procedures conformed to the standards set by the latest revision of the Declaration of Helsinki and the study protocol was approved by the Research Ethics Committee of the "Institut Universitaire de Gériatrie de Montréal".

2.2. Painful electrical stimulation

Transcutaneous electrical stimulation was delivered with a Grass S48 square pulse stimulator (Astro-Med) through a constant-current stimulus-isolation unit and a radio-frequency (RF) filter. The stimulation consisted in a 30 ms train of 10 × 1 ms pulse, delivered on degreased skin over the retromalleolar path of the right sural nerve using a pair of surface Ag/AgCl electrodes (diameter 8 mm; Biopac EL258RT, Biopac Systems) with an interelectrode distance of 15 mm. The NFR was assessed similarly as in prior studies (Piché et al., 2010, 2009).

2.3. fMRI acquisition

Imaging data was acquired at the "Unité de Neuroimagerie Fonctionnelle" of the "Centre de recherche de l'Institut de gériatrie de Montréal" on a 3T Siemens Trio scanner using a CP head coil. The head of the subject was stabilized in a comfortable position using a vacuum bag. Subjects were instructed to refrain from moving as much as possible throughout the imaging session and were given earplugs to reduce the noise from the scanner. A pelvic belt stabilizing the subjects on the table of the scanner at the level of the iliac crest was used to limit the potential movements induced by the NFR. The functional scans were collected using a blood oxygen level-dependent (BOLD) protocol with a T2*-weighted gradient echo-planar imaging sequence (TR: 3.0 s with an intervolume delay of 500 ms; TE: 30 ms; flip angle: 90°; 64 × 64 matrix; 445 vol acquisitions). Electrical stimulations were always administered during the intervolume delay, thereby avoiding the potential contamination of fMRI images by shock-induced artifacts and of EMG recordings of the NFR by RF-pulse artifacts. The scanning planes were oriented with a backward tilt of 15° from the anterior–posterior commissure line and covered the entire brain from the vertex of the cortex to the lower brain stem (39 contiguous 3.5-mm-thick slices; voxel size, 3.5 × 3.5 × 3.5 mm). Each participant also underwent one high-resolution anatomical scan between the two runs of functional scans (see below). The anatomical scan was a T1-weighted high-resolution scan using a turbo FLASH sequence [repetition time (TR): 2300 ms; echo time (TE): 2.98 ms; time to inversion (TI): 900 ms; flip angle: 9°; voxel size: 1 × 1 × 1 mm; 176 slices].

2.4. Experimental paradigm

Before the scanning session, participants were installed in a scanner simulator, received the instructions for the high and the low demanding conditions of the counting Stroop task (Bush et al., 1998) and had 16 practice trials in each condition to familiarize themselves with the experimental task and the response key. Participants were informed that they would see sets of one to four identical words presented vertically on the screen. They were asked to report the number of words presented on the screen using the buttons of the keyboard as quickly and accurately as possible, with an emphasis placed on not sacrificing accuracy for speed. Moreover, participants were asked not to blur their vision to make the counting task easier. In the high demanding condition, the words were the number words "one", "two", "three", and "four"—presented in French ("un", "deux", "trois", "quatre")—that were always displayed a different number of times than their respective meaning (e.g. two times the words "three"). The interference between reading and counting the words commonly requires cognitive control to override the automatic response of reading and to provide the right answer. In the low demanding condition, the presented words were neutral words matched in length with the number words: "an", "drap", "table", and "quille"—which respectively mean in English "year", "sheet", "table", and "skittle". Words were presented in capital letters in the font *Verdana* size 20. Trials started with a fixation cross (1000 ms) followed by the words to count which stayed on the screen until the participants gave their response but not more than 1250 ms. During the practice trials, participants received correctness feedback and were asked to answer more quickly if they did not provide an answer within the time limit. Once these practice trials were completed, participants were installed on the scanner bed and electrodes were attached.

First, the individual NFR threshold was determined using the staircase method, involving several series of ascending– descending intensities administered until a stable threshold was obtained (typically 50 stimuli). For the experimental conditions (see below), the stimulation

intensity was adjusted to 120% of the threshold ($M = 11.32$ mA; $SD = 3.66$) and remained constant throughout the scanning experiment.

Then, participants were moved inside the scanner and two functional scanning runs of 22 min each were conducted, separated by the anatomical scan. Both scanning runs began with four electrical stimulations at 120% of the threshold with inter-stimulation intervals varying randomly between 3 and 9 s. After the four stimulations, participants rated the overall pain intensity and unpleasantness felt using a cursor displayed on the screen over the visual-analog scales (VAS's) and controlled with the middle and index fingers. The scales ranged from *No pain/Not unpleasant at all* (0) to *The most intense/unpleasant pain imaginable* (100). These four stimulations were administered to control for the rapid habituation effect observed occasionally on the first few trials of a series of NFR measurements.

Then participants performed blocks of 32 experimental trials of the counting Stroop task always with a neutral feedback ("response entered"). The feedback appeared for 2 s minus participants' reaction time, assuring that all trials (3.4 s) and all blocks (2 min) had the same length. Inter-trial intervals varied randomly (2–5 s). Each participant performed two consecutive blocks in the low demand condition and two consecutive blocks in the high demand condition which were separated by a short break of 30 s. Half of the participants ($n = 12$, 8 females, 4 males) started with the low demand condition and the other half ($n = 12$, 8 females, 4 males) with the high demand condition.

Following the last trial of each block, four electrical stimulations were administered at 120% of the previously defined NFR threshold with inter-stimulation intervals varying randomly between 3, 6, and 9 s (Fig. 1a). After the fourth stimulation, participants rated the overall intensity and unpleasantness of pain felt (total rating time allowed: 24sec). Then participants waited 10 s before the next block started. At the end of each condition—i.e., after the second block—participants also rated two items of perceived task difficulty ("How difficult was the task?" and "How difficult was it for you to achieve the task successfully?"; *Not at all* [0] to *Very difficult* [10]), and one item related to task engagement ("Did you try to answer correctly and rapidly until the end of the task?"; *Not at all* [0] to *Very much* [10]). Finally, four electrical stimulations at 120% of the threshold were administered after a break of 2 min and pain ratings assessed to obtain a second habituation control measurement at the end

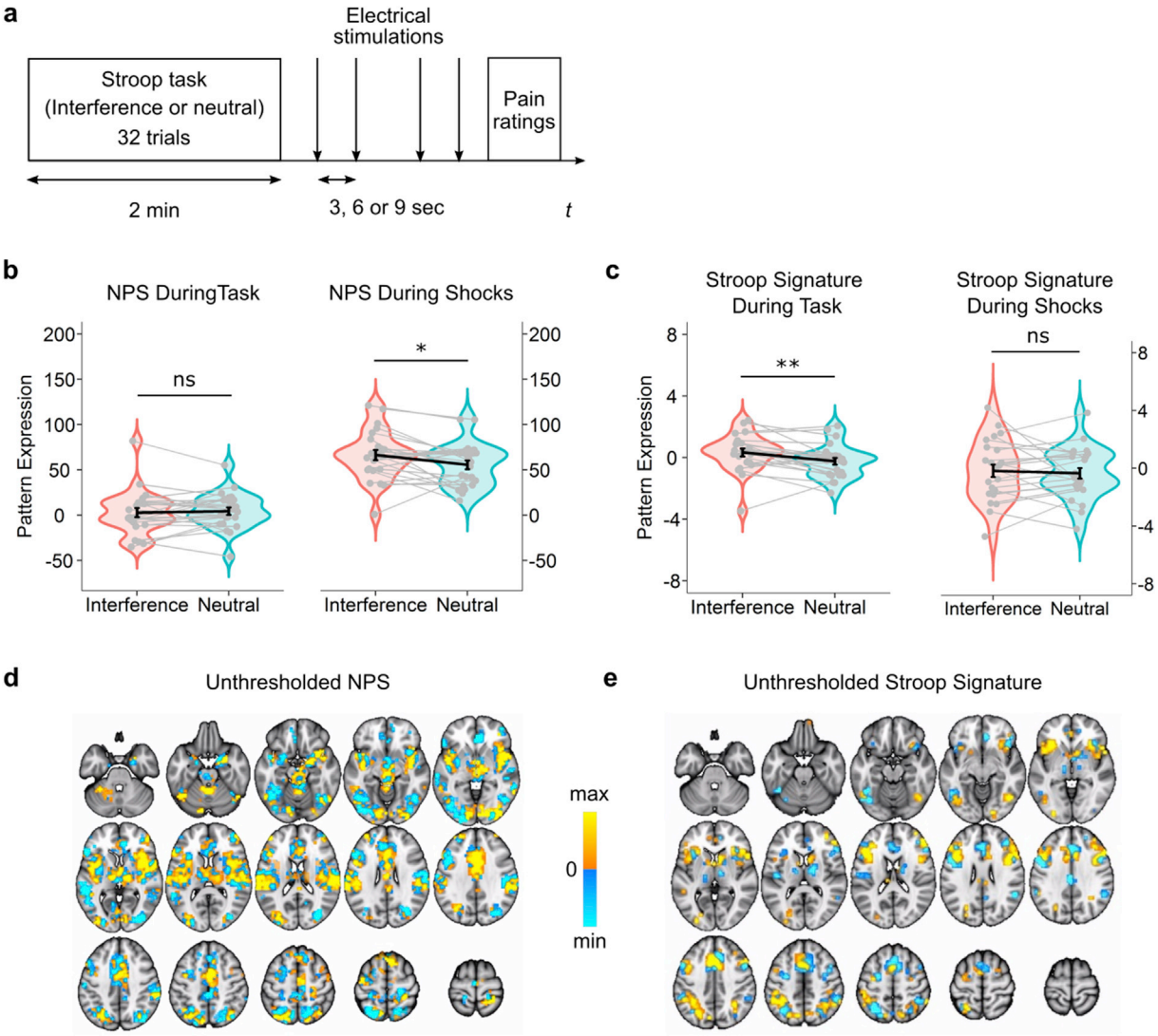

Fig. 1. Experimental procedure and fMRI pattern analyses. Panel **(a)** shows the details of one experimental block constituted by 2 min of the Stroop task either in the interference or in the neutral condition followed by four electrical stimulations and pain ratings. The black lines and error bars represent means and standard errors of pattern expression for (**b**) the Neurological Pain Signature (NPS) and (**c**) the task pattern during the Stroop task and the shocks in the high and the low demanding conditions. Grey dots and lines represent individual participants. $^{*}P < .05$, $^{**}P < .01$, one-tailed, paired *t*-test. Unthresholded patterns of (**d**) the Neurological Pain Signature (NPS) and (**e**) the task pattern predictive weights. These unthresholded pattern maps included both positive (orange/yellow) and negative (blue) weights and were used to investigate pattern expression of brain activity during the Stroop task and during the shocks.

of the scanning run. There were no significant differences between habituation and experimental pain measurements (pain ratings and NFR; *ps* > .12). Therefore, habituation pain measurements obtained at the beginning and at the end of each run were not included in the following analyses of experimental pain ratings and NFR.

The anatomical scan was then completed and the second run started, which was similar to the first run with a reversed order of experimental conditions. A total of 48 electrical stimulations were therefore administered during the two scanning runs. Visual stimuli and rating scales were presented on a computer monitor back projected onto a screen and viewed on a mirror placed on the head coil in front of the participant's eyes using a script running in Eprime 2.0 (Psychology Software Tools Inc., Pittsburgh, PA, USA), which also triggered the electrical stimulations.

2.5. NFR and pain ratings analyses

EMG data was analyzed similarly as in previous studies (Piché et al., 2010, 2009). To exclude potential erroneous measurements, NFR values exceeding two standard deviations from the mean of each participant were replaced by missing values. Mean NFR was then calculated for each experimental condition by averaging the corresponding integrated values (Cronbach's αs > 0.85). NFR data of four participants were excluded from the analyses due to technical problems and noisy EMG signals. Given that the nociceptive flexion reflex was not affected by the experimental manipulation (P > .38), these results are not further discussed.

Preliminary analyses on pain ratings revealed non-normal distributions (Kolmogorov-Smirnov tests, *ps* < .001) due to two extreme values (<2SD from the mean) in the effect of the experimental manipulation. Therefore, pain scores were analyzed using robust t-tests based on iteratively reweighted least-square (IRLS) (Wager et al., 2005). NFR scores, average number of errors during the task, reaction times, and manipulation checks were analyzed using paired-sample *t*-tests one-tailed due to our clear a priori hypotheses. According to preliminary analyses, sex, order of condition presentation, and the time variable related to the two consecutive runs did not interact significantly with the experimental conditions regarding pain measurements and were therefore not considered in the main analyses. Moreover, variances did not differ significantly for all dependent variables in both groups of subjects in the two different orders according to Levene's test (*ps* > .05).

2.6. fMRI data analyses

Brain imaging data were analyzed using SPM8 (Wellcome Department of Cognitive Neurology, London, UK; http://www.fil.ion.ucl.ac.uk/spm/). Preprocessing included slice-time correction and realignment for movement correction. Anatomical and functional images were spatially normalized to a standard stereotaxic space using the Montreal Neurological Institute (MNI) template. Subsequently, functional images were spatially smoothed using a Gaussian kernel of twice the voxel size (FWHM: 7 × 7 × 7 mm), temporally filtered using a high-pass filter with a cutoff period of 256 s (the high-pass filter cutoff period was adjusted according to the time frequencies of our experimental conditions), and were corrected for serial autocorrelation using the AR(1) correction implemented in SPM.

2.6.1. First-level fMRI analyses

The effects of interest were assessed using general linear models including both scanning runs. First, individual contrasts were generated using a mixed-design model. The 24 electric stimulations in each run were assigned to six event-related conditions: (1) habituation shocks at the beginning of the experience, (2) habituation shocks at the end of the experience, (3) shocks following the first block of the high demand condition, (4) shocks following the second block of the high demand condition, (5) shocks following the first block of the low demand condition, and (6) shocks following the second block of the low demand condition. The items of the task were assigned to four event-related conditions: items of the first (n = 32) and second block (n = 32) of the high demand condition and items of the first (n = 32) and second (n = 32) block in the low demand condition (n = 32). We also included in the model, vectors related to pain ratings as 6 blocks of 27 s and to the manipulation-check questions as 2 blocks of 36 s. These 18 vectors were convolved with a canonical hemodynamic response function. In addition, motion-correction parameters from the realignment procedure were entered as six regressors of no interest to remove potential movement-related variance (maximum instantaneous movement tolerated in all subjects < 3 mm and <3°). Finally, two vectors integrating the mean signals of regions including white matter and cerebrospinal fluid (determined from the segmentation procedure) were also entered as two regressors of no interest to remove noise-related variance. Voxel-wise statistical parametric maps for shock-evoked activity after the high demand vs. after the low demand condition and changes in task-related activity between the high and the low demand condition were calculated for each participant and then entered into MVPA.

2.6.2. Multivariate voxel pattern analyses

We computed the dot products of the brain activity related to our two experimental conditions during the task and during the shocks within two different masks. First, we used a mask including a distributed pattern of pain-related brain areas—the Neurological Pain Signature (NPS)—that was elaborated and validated across four fMRI studies showing overall that the strength of the NPS discriminated various levels of reported pain and was specific for physical pain (Wager et al., 2013). Second, we used a mask including a distributed pattern of brain areas related to the Stroop task. A priori voxels associated with the term 'Stroop' were selected based on the union of forward and reverse inference maps from an automated large-scale meta-analytic database of more than 5800 published neuroimaging studies (http://neurosynth.org22).

2.6.3. Focused analyses on aMCC

We used linear support vector machines (SVMs) (Vapnik, 2013) to train multivariate pattern classifiers within aMCC for the task and the shocks. The task-related aMCC mask corresponded to an a priori meta-analytic map including aMCC activity induced by pain, cognitive control, and negative affect (Shackman et al., 2011) (data retrieved from http://neurovault.org). The shock-related aMCC mask consisted of the conjunction of the previous meta-analytic map with the NPS to obtain an aMCC subregion of the NPS. The SVMs were implemented using custom Matlab code based on the Spider toolbox (http://people.kyb.tuebingen.mpg.de/spider). The pattern classifiers were trained on first-level contrast images for the two experimental conditions to discriminate the high and the low demand condition during the task and during the shocks.

2.6.4. Mediation analysis

To examine the mediating role of aMCC task-pattern response during the shocks in the effect of the aMCC task-pattern response during the task on aMCC-NPS response during the shocks, a mediation analysis was performed using the Mediation Toolbox written in Matlab (mediation.m available at https://github.com/canlab/MediationToolbox). More technical details on mediation analyses implemented in the Mediation Toolbox can be found in previous reports (Wager et al., 2008; Woo et al., 2015). In the current study, aMCC task-pattern response during the task was entered as a predictor (X), aMCC-NPS response during the shocks as an outcome variable (Y) and aMCC task-pattern response during the shocks as a mediator (M). Bootstrap tests (10,000 iterations) were used for significance testing of mediation effects.

3. Results

3.1. Behavioral data

As expected, participants were slower when performing the more demanding cognitive task (732.20 ± 12.66 [mean ± standard error] vs. 712.50 ± 12.16, $t[23] = 3.98$, $P < .001$, $r = 0.63$) and made more errors (1.91% ± 0.34 vs. 1.30% ± 0.23, $t[23] = 2.06$, $P < .025$, $r = 0.40$), indicating higher demand on cognitive control processes. Moreover, the more demanding condition was perceived as more difficult than the low demand condition (1.82 ± 0.33 vs. 1.38 ± 0.28, $t[23] = 3.10$, $P = .003$, $r = 0.29$). Drawing on the hypothesis of impaired regulatory mechanisms after demanding tasks, we expected greater pain perception after high than after low cognitive demand. Crucially, this was indeed the case: although the difference was small in absolute magnitude, within-subject comparisons confirmed that pain was rated as significantly more intense (38.80 ± 4.97 vs. 38.12 ± 4.65, robust $t[23] = 2.39$, $P = .013$, $r = 0.20$) and more unpleasant (42.87 ± 4.92 vs. 41.76 ± 5.18, robust $t[23] = 4.13$, $P < .001$, $r = 0.43$) after the high than after the low demand condition.

3.2. fMRI pattern analyses

Brain imaging data revealed stronger shock-related NPS response after high than low cognitive demand ($t[23] = 2.34$, $P = .014$, $r = 0.44$), confirming stronger pain-related brain activity after exertion of cognitive control (Fig. 1b). Importantly, NPS response did not differ between conditions *during* the Stroop task ($P > .31$). In contrast, the task pattern response was stronger in the high demand than in the low demand condition during Stroop performance ($t[23] = 2.92$, $P = .004$, $r = 0.52$), whereas it was not different between conditions in response to the painful stimuli ($P > .31$; Fig. 1c). This double dissociation suggests that two distinct brain systems (Fig. 1d and e) are separately modifiable by pain and cognitive control (Sternberg, 2001): The NPS responds only to painful stimuli during pain, whereas the task-related pattern responds only to cognitive demand during Stroop performance. This validates the patterns as markers for pain and cognitive demand, respectively. Given this validation, the effects of previous cognitive demand on pain and NPS responses during pain can be interpreted as effects of cognitive demand on pain-related brain responses.

3.3. Focus on aMCC

Further analyses focusing on the NPS local pattern within the aMCC region (aMCC-NPS pattern) revealed similar results as for the whole NPS. The local aMCC-NPS pattern showed stronger shock-related activity after high than low task demands ($t[23] = 2.19$, $P = .019$, $r = 0.17$), but showed no effect of cognitive demand *during* Stroop performance ($P > .92$; Fig. 2a). In contrast, a cognitive demand-related aMCC pattern—trained to discriminate the high vs. low demand conditions—responded more strongly to high vs. low cognitive demand *both* during Stroop performance ($t[23] = 3.20$, $P = .002$, $r = 0.55$; Fig. 2b) and during subsequent shocks ($t[23] = 5.19$, $P < .001$, $r = 0.73$). The carry-over response during shocks could indicate that the aMCC task pattern is less selective than the whole-brain pattern. It may also be a substrate for interactions between task- and pain-related processes—specifically, the reactivation of task-related neural networks may perturb overlapping networks underlying spontaneous pain regulatory functions, thereby increasing pain-related responses. Unthresholded aMCC-NPS and aMCC task patterns are presented in Fig. 2c and d, respectively.

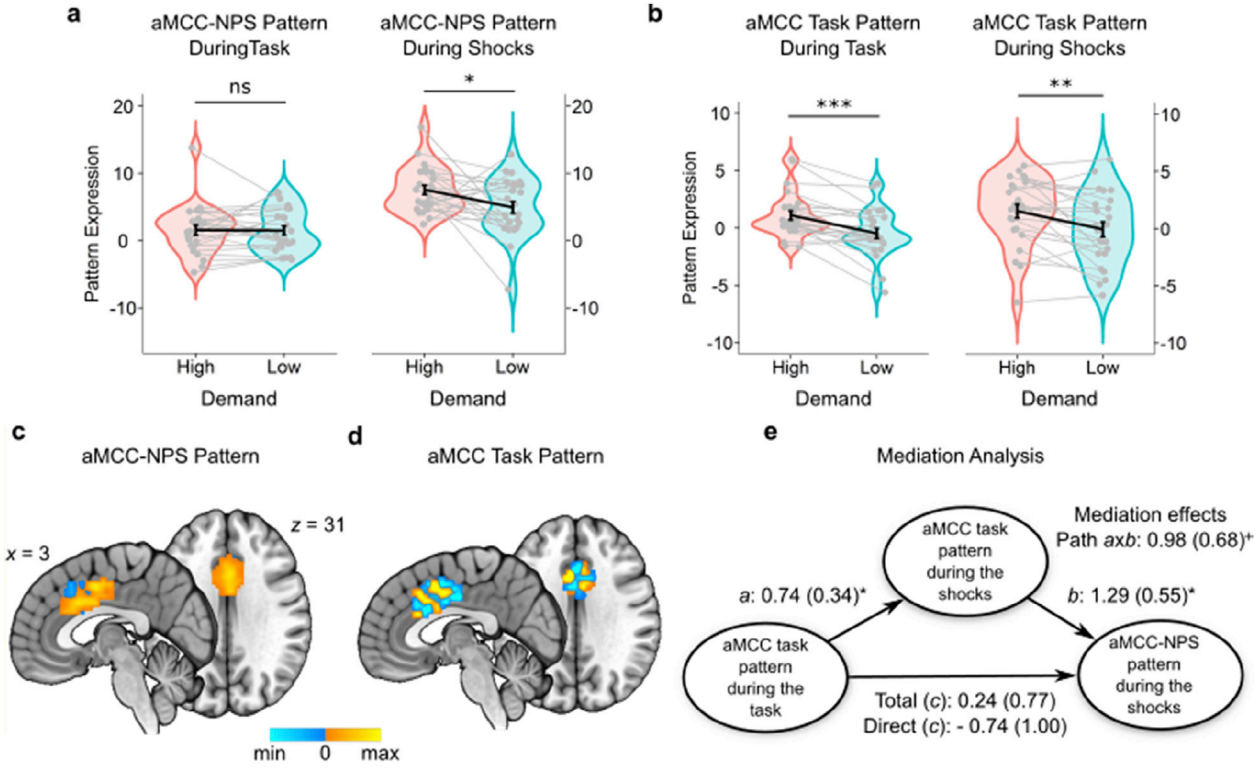

Fig. 2. Focus on aMCC. The black lines and error bars represent means and standard errors of pattern expression for (**a**) the NPS local pattern within the aMCC region (aMCC-NPS pattern) and (**b**) the aMCC task pattern, developed to discriminate between the high and the low demanding conditions (aMCC task pattern), during the Stroop task and the shocks in the high and the low demanding conditions. Grey dots and lines represent individual participants. *$P < .05$, **$P < .01$, ***$P < .001$, one-tailed, paired *t*-test. Classifier voxel weights within the aMCC (positive weights in orange/yellow and negative weights in blue) determined by trained linear support vector machines (SVMs) and that reliably discriminated the high and the low demanding conditions during the shocks (**c**) and during the Stroop (**d**). Mediation analysis (**e**) showing that aMCC task pattern responses during the shocks mediated the relationship between aMCC task pattern responses during the Stroop and aMCC-NPS pattern responses during the shocks. $^{+}P < .07$, *$P < .05$, one-tailed, bootstrap test.

Potential mechanisms underlying the interaction between task- and pain-responses were further tested using mediation analysis (Atlas et al., 2010). Results suggested an after-effect of cognitive control where the aMCC task-pattern was partly reactivated in response to the shock (i.e. carry-over effect; see Fig. 2e, path a). Moreover, this increased aMCC task-pattern responses to the shocks also predicted an increase in aMCC-NPS responses to the shocks (path *b*), and mediated the effect of aMCC task-pattern responses during the task on aMCC-NPS responses to the shocks (path *ab*). Even when the whole brain NPS response was used as an outcome variable, the aMCC task-pattern response during the shocks was a significant mediator ($\widehat{\beta} = 3.6$, $P = .040$, one-tailed, bootstrap test), showing that the task after-effect impacts the distributed pain-response beyond the aMCC.

4. Discussion

The present findings offer support to our hypothesis that engaging cognitive control in a first task leads to impaired regulatory mechanisms and increases in subsequent pain responses. Participants reported more intense and more unpleasant pain after performing a task with high cognitive demand than low demand. Moreover, increases in pain-related brain activity in the NPS responses after high compared to low demand further supported this effect. Focused analyses on aMCC indicated that increases in aMCC task-related activation pattern during pain predicted increases in pain-related local aMCC and whole brain activation patterns, which we interpret as a neural correlate of the after-effect of cognitive control on pain.

Behavioral effects are in line with previous findings showing decreased pain tolerance and increases in pain responses following demanding tasks (Silvestrini and Rainville, 2013; Vohs et al., 2008). In the framework of the so-called ego-depletion effect (Baumeister et al., 2018, 2007, 1998), these findings suggest that both cognitive control and pain rely on common and limited functional resources. According to this view, performing a demanding cognitive task temporarily decreases self-regulatory capacity, which leads to increases in subsequent pain perception. Importantly, it is of note that accumulating evidence indicates that the subjective perception of reduced self-regulatory capacity might be more determinant in these effects than the depletion of some biological resource (Clarkson et al., 2010; Job et al., 2010). As noted earlier, the precise mechanisms underlying these effects and even the validity of such effects are still highly debated (Baumeister et al., 2018; Hagger and Chatzisarantis, 2016). Here, the present findings offer support to the behavioral predictions and insights into potential neural mechanisms as described below.

Using multivariate pattern analyses, we found that exerting cognitive control leads to increases in pain-related brain activity in the NPS, a distributed pattern of fMRI activity previously shown to be sensitive and specific to nociceptive pain (Wager et al., 2013). As visible in Fig. 1d, the NPS mainly includes the thalamus, the posterior and anterior insulae, the secondary somatosensory cortex, the anterior cingulate cortex, and the periaqueductal grey matter. This finding offers additional support to the predicted after-effect of cognitive control on pain by showing an impact of the demanding task on subsequent pain-related brain activation. Importantly, the NPS did not differ between conditions during task performance whereas a global brain activation pattern developed to discriminate the high and low demanding task only responded to cognitive demand during Stroop performance and did not differ during shocks. This reveals distinct and dissociable brain systems separately modifiable by pain and cognitive control (Sternberg, 2001) and validates the patterns as markers for pain and cognitive demand, respectively. As visible in Fig. 1e, the task-related activation pattern mainly includes the anterior cingulate cortex, the anterior insula, lateral prefrontal areas, and posterior areas.

Previous studies on the neural mechanisms underlying the ego-depletion effect found that self-regulatory failures mainly emerge due to impaired top-down control following self-control exertion in areas such as the dorsolateral and ventrolateral prefrontal cortices (DLPFC, VLPFC), the dorsal anterior cingulate cortex (dACC), and the lateral parietal cortex (Friese et al., 2013; Inzlicht et al., 2016). Further research showed that impairment in top-down control in turn lead to increased activity in areas processing the specific domain engaged during self-regulatory failure, e.g. amygdala and orbitofrontal cortex for responses to negative emotional scenes and unhealthy food pictures viewing, respectively (Wagner et al., 2013; Wagner and Heatherton, 2012). Moreover, these studies revealed diminished functional connectivity between the DLPFC and the respective reactivity regions suggesting that depletion uncouples top-down control from emotional reactivity.

In the present study, we report a different kind of mechanism related to local pattern activation within the aMCC. Focused analyses on the aMCC revealed a reactivation of the aMCC task pattern to the shocks, which led to stronger pain response in the aMCC and in the whole NPS pattern. This suggests an after-effect of local aMCC activation pattern related to cognitive control on subsequent pain-related brain activation. We interpret this finding in the light of previous evidence on aMCC as a common region engaged in various domains. A recent meta-analysis and review of anatomical studies indicates that pain, cognitive control, and also interestingly negative affect consistently activate the aMCC, which may reflect control processes that are common to all three domains (Shackman et al., 2011). The authors of this meta-analysis propose that the aMCC implements adaptive control by integrating information about punishment to determine an optimal course of action in the face of uncertainty. Our findings indicate that although both cognitive control and pain activate the aMCC, distinct aMCC activation patterns are associated with these two domains and that these patterns interact leading to an after-effect of cognitive control on pain. This suggests that the (re)activation of neural networks associated with cognitive control may perturb local pain-related regulatory networks within the aMCC, leading to increased nociceptive responses. Therefore, this carry-over effect may reflect persisting processes related to the demanding task that temporarily impair subsequent regulatory mechanisms. These persisting processes might contribute to the reduction of self-regulatory capacity after demanding tasks.

To conclude, our findings offer insights into the issue of aMCC functional specificity (Critchley, 2004; Lieberman and Eisenberger, 2015; Shenhav et al., 2016; Wager et al., 2016). Accumulating evidence shows aMCC activation in different domains such as pain (Rainville et al., 1997), social rejection (Lieberman and Eisenberger, 2015), cognitive control (Botvinick et al., 2001), value-based decision making (Shenhav et al., 2016), and negative affect (Ochsner and Gross, 2005). Therefore, it seems hardly tenable to claim that aMCC should be specific to one of these (Wager et al., 2016). However, the present study shows the activation of distinct patterns within this region during cognitive control and pain suggesting that specific local networks or neuronal population codes may be engaged in each phenomenon (see Peelen et al., 2006; Woo et al., 2014). A recent study revealed similar findings by showing distinct medial frontal cortex representations specific to pain, cognitive control, and negative emotions (Kragel et al., 2018). Therefore, further studies investigating local patterns within the aMCC may contribute to disentangle the functional specificity of this region in different domains beyond common fMRI activity at the gross anatomical level.

Declaration of competing interest

The authors declare no competing financial interests.

CRediT authorship contribution statement

Nicolas Silvestrini: Funding acquisition, Conceptualization, Methodology, Investigation, Formal analysis, Visualization, Writing - original draft, Writing - review & editing. **Jen-I Chen:** Data curation, Software, Formal analysis, Visualization, Writing - review & editing. **Mathieu Piché:** Methodology, Investigation, Formal analysis, Writing - review &

editing. **Mathieu Roy:** Formal analysis, Writing - review & editing. **Etienne Vachon-Presseau:** Methodology, Investigation, Writing - review & editing. **Choong-Wan Woo:** Software, Formal analysis, Visualization, Writing - review & editing. **Tor D. Wager:** Software, Formal analysis, Resources, Writing - review & editing. **Pierre Rainville:** Funding acquisition, Supervision, Resources, Conceptualization, Methodology, Writing - review & editing.

Acknowledgment

We thank Nadine LeBlanc and Anouk Streff for their help in the recruitment and installation of the participants, Carollyn Hurst and André Cyr from the *Unité de neuroimagerie fonctionnelle* of the *Institut Universitaire de Gériatrie de Montréal*, and Suzie Bois for her help in the processing of EMG data. This research was funded by an operating grant of the Canadian Institute of Health Research (Canada) awarded to P.R., E.V.P., M.P. and M.R. (MOP#130341) and by a grant awarded to N.S. from the Swiss National Science Foundation (PBGEP1-131388, Switzerland). P.R. received salary support from the Fonds de la Recherche Québec – Santé (FRQS). The authors have no conflicts of interest to report. Correspondence concerning this article should be addressed to Nicolas Silvestrini, Faculty of Psychology and Educational Sciences, Section of Psychology, University of Geneva, Boulevard du Pont-d'Arve 40, CH-1211 Geneva 4, Switzerland. E-mail: nicolas.silvestrini@unige.ch.

References

Bush, G., Whalen, P.J., Rosen, B.R., Jenike, M.A., McInerney, S.C., Rauch, S.L., 1998. The counting stroop: an interference task specialized for functional neuroimaging-validation study with functional MRI. Hum. Brain Mapp 6, 270–282. https://doi.org/10.1002/(SICI)1097-0193(1998)6:4<270::AID-HBM6>3.0.CO;2–0.

Atlas, L.Y., Bolger, N., Lindquist, M.A., Wager, T.D., 2010. Brain mediators of predictive cue effects on perceived pain. J. Neurosci. 30, 12964.

Baumeister, R.F., Bratslavsky, E., Muraven, M., Tice, D.M., 1998. Ego depletion: is the active self a limited resource? J. Pers. Soc. Psychol. 74, 1252–1265. https://doi.org/10.1037/0022-3514.74.5.1252.

Baumeister, R.F., Vohs, K.D., Tice, D.M., 2007. The strength model of self-control. Curr. Dir. Psychol. Sci. 16, 351–355. https://doi.org/10.1111/j.1467-8721.2007.00534.x.

Baumeister, R.F., Tice, D.M., Vohs, K.D., 2018. The strength model of self-regulation: conclusions from the second decade of willpower research. Perspect. Psychol. Sci. 13, 141–145. https://doi.org/10.1177/1745691617716946.

Botvinick, M.M., Braver, T.S., Barch, D.M., Carter, C.S., Cohen, J.D., 2001. Conflict monitoring and cognitive control. Psychol. Rev. 108, 624–652. https://doi.org/10.1037/0033-295X.108.3.624.

Buhle, J., Wager, T.D., 2010. Performance-dependent inhibition of pain by an executive working memory task. Pain 149, 19–26. https://doi.org/10.1016/j.pain.2009.10.027.

Bush, G., Luu, P., Posner, M.I., 2000. Cognitive and emotional influences in anterior cingulate cortex. Trends Cognit. Sci. 4, 215–222. https://doi.org/10.1016/S1364-6613(00)01483-2.

Clarkson, J.J., Hirt, E.R., Jia, L., Alexander, M.B., 2010. When perception is more than reality: the effects of perceived versus actual resource depletion on self-regulatory behavior. J. Pers. Soc. Psychol. 98, 29–46. https://doi.org/10.1037/a0017539.

Critchley, H.D., 2004. The human cortex responds to an interoceptive challenge. Proc. Natl. Acad. Sci. U.S.A. 101, 6333–6334. https://doi.org/10.1073/pnas.0401510101.

Davis, K.D., Taylor, S.J., Crawley, A.P., Wood, M.L., Mikulis, D.J., 1997. Functional MRI of pain- and attention-related activations in the human cingulate cortex. J. Neurophysiol. 77, 3370–3380.

Eccleston, C., Crombez, G., 1999. Pain demands attention: a cognitive-affective model of the interruptive function of pain. Psychol. Bull. 125, 356–366. https://doi.org/10.1037/0033-2909.125.3.356.

Friese, M., Binder, J., Luechinger, R., Boesiger, P., Rasch, B., 2013. Suppressing emotions impairs subsequent stroop performance and reduces prefrontal brain activation. PloS One 8, e60385. https://doi.org/10.1371/journal.pone.0060385.

Hagger, M.S., Chatzisarantis, N.L.D., 2016. A multilab preregistered replication of the ego-depletion effect. Perspect. Psychol. Sci. 11, 546–573. https://doi.org/10.1177/1745691616652873.

Hagger, M.S., Wood, C., Stiff, C., Chatzisarantis, N.L.D., 2010. Ego depletion and the strength model of self-control: a meta-analysis. Psychol. Bull. 136, 495–525. https://doi.org/10.1037/a0019486.

Haxby, J.V., Gobbini, M.I., Furey, M.L., Ishai, A., Schouten, J.L., Pietrini, P., 2001. Distributed and overlapping representations of faces and objects in ventral temporal cortex. Science 293, 2425–2430. https://doi.org/10.1126/science.1063736.

Inzlicht, M., Schmeichel, B.J., 2012. What is ego depletion? Toward a mechanistic revision of the resource model of self-control. Perspect. Psychol. Sci. 7, 450–463. https://doi.org/10.1177/1745691612454134.

Inzlicht, M., Berkman, E., Elkins-Brown, N., 2016. The neuroscience of "ego depletion". How the brain can help us understand why self-control seems limited. In: Harmon-Jones, E., Inzlicht, M. (Eds.), Social Neuroscience: Biological Approaches to Social Psychology. New York, pp. 1–44.

Job, V., Dweck, C.S., Walton, G.M., 2010. Ego depletion—is it all in your head? Implicit theories about willpower affect self-regulation. Psychol. Sci. 21, 1686–1693. https://doi.org/10.1177/0956797610384745.

Kool, W., Botvinick, M., 2014. A labor/leisure tradeoff in cognitive control. J. Exp. Psychol. Gen. 143, 131–141. https://doi.org/10.1037/a0031048.

Kragel, P.A., Kano, M., Oudenhove, L.V., Ly, H.G., Dupont, P., Rubio, A., Delon-Martin, C., Bonaz, B.L., Manuck, S.B., Gianaros, P.J., Ceko, M., Losin, E.A.R., Woo, C.-W., Nichols, T.E., Wager, T.D., 2018. Generalizable representations of pain, cognitive control, and negative emotion in medial frontal cortex. Nat. Neurosci. 21, 283–289. https://doi.org/10.1038/s41593-017-0051-7.

Kurzban, R., Duckworth, A., Kable, J.W., Myers, J., 2013. An opportunity cost model of subjective effort and task performance. Behav. Brain Sci. 36, 661–679. https://doi.org/10.1017/S0140525X12003196.

Legrain, V., Van Damme, S., Eccleston, C., Davis, K.D., Seminowicz, D.A., Crombez, G., 2009. A neurocognitive model of attention to pain: behavioral and neuroimaging evidence. Pain 144, 230–232. https://doi.org/10.1016/j.pain.2009.03.020.

Lieberman, M.D., Eisenberger, N.I., 2015. The dorsal anterior cingulate cortex is selective for pain: results from large-scale reverse inference. Proc. Natl. Acad. Sci. U.S.A. 112, 15250–15255. https://doi.org/10.1073/pnas.1515083112.

Ochsner, K.N., Gross, J.J., 2005. The cognitive control of emotion. Trends Cognit. Sci. 9, 242–249. https://doi.org/10.1016/j.tics.2005.03.010.

Peelen, M.V., Wiggett, A.J., Downing, P.E., 2006. Patterns of fMRI activity dissociate overlapping functional brain areas that respond to biological motion. Neuron 49, 815–822. https://doi.org/10.1016/j.neuron.2006.02.004.

Piché, M., Arsenault, M., Rainville, P., 2009. Cerebral and cerebrospinal processes underlying counterirritation analgesia. J. Neurosci. 29, 14236–14246. https://doi.org/10.1523/JNEUROSCI.2341-09.2009.

Piché, M., Arsenault, M., Rainville, P., 2010. Dissection of perceptual, motor and autonomic components of brain activity evoked by noxious stimulation. Pain 149, 453–462. https://doi.org/10.1016/j.pain.2010.01.005.

Rainville, P., Duncan, G.H., Price, D.D., Carrier, B., Bushnell, M.C., 1997. Pain affect encoded in human anterior cingulate but not somatosensory cortex. Science 277, 968–971. https://doi.org/10.1126/science.277.5328.968.

Shackman, A.J., Salomons, T.V., Slagter, H.A., Fox, A.S., Winter, J.J., Davidson, R.J., 2011. The integration of negative affect, pain and cognitive control in the cingulate cortex. Nat. Rev. Neurosci. 12, 154–167. https://doi.org/10.1038/nrn2994.

Shenhav, A., Cohen, J.D., Botvinick, M.M., 2016. Dorsal anterior cingulate cortex and the value of control. Nat. Neurosci. 19, 1286–1291. https://doi.org/10.1038/nn.4384.

Silvestrini, N., Rainville, P., 2013. After-effects of cognitive control on pain. Eur. J. Pain 17, 1225–1233. https://doi.org/10.1002/j.1532-2149.2013.00299.x.

Sternberg, S., 2001. Separate modifiability, mental modules, and the use of pure and composite measures to reveal them. Acta Psychol., Looking for stages 106, 147–246. https://doi.org/10.1016/S0001-6918(00)00045-7.

Vapnik, V., 2013. The Nature of Statistical Learning Theory. Springer Science & Business Media.

Vohs, K.D., Baumeister, R.F., Schmeichel, B.J., Twenge, J.M., Nelson, N.M., Tice, D.M., 2008. Making choices impairs subsequent self-control: a limited-resource account of decision making, self-regulation, and active initiative. J. Pers. Soc. Psychol. 94, 883–898. https://doi.org/10.1037/0022-3514.94.5.883.

Wager, T.D., Keller, M.C., Lacey, S.C., Jonides, J., 2005. Increased sensitivity in neuroimaging analyses using robust regression. Neuroimage 26, 99–113. https://doi.org/10.1016/j.neuroimage.2005.01.011.

Wager, T.D., Davidson, M.L., Hughes, B.L., Lindquist, M.A., Ochsner, K.N., 2008. Prefrontal-subcortical pathways mediating successful emotion regulation. Neuron 59, 1037–1050. https://doi.org/10.1016/j.neuron.2008.09.006.

Wager, T.D., Atlas, L.Y., Lindquist, M.A., Roy, M., Woo, C.-W., Kross, E., 2013. An fMRI-based neurologic signature of physical pain. N. Engl. J. Med. 368, 1388–1397. https://doi.org/10.1056/NEJMoa1204471.

Wager, T.D., Atlas, L.Y., Botvinick, M.M., Chang, L.J., Coghill, R.C., Davis, K.D., Iannetti, G.D., Poldrack, R.A., Shackman, A.J., Yarkoni, T., 2016. Pain in the ACC? Proc. Natl. Acad. Sci. U.S.A. 113, E2474–E2475. https://doi.org/10.1073/pnas.1600282113.

Wagner, D.D., Heatherton, T.F., 2012. Self-regulatory depletion increases emotional reactivity in the amygdala. Soc. Cognit. Affect Neurosci. 410–417. https://doi.org/10.1093/scan/nss082.

Wagner, D.D., Altman, M., Boswell, R.G., Kelley, W.M., Heatherton, T.F., 2013. Self-regulatory depletion enhances neural responses to rewards and impairs top-down control. Psychol. Sci. 24, 2262–2271. https://doi.org/10.1177/0956797613492985.

Woo, C.-W., Koban, L., Kross, E., Lindquist, M.A., Banich, M.T., Ruzic, L., Andrews-Hanna, J.R., Wager, T.D., 2014. Separate neural representations for physical pain and social rejection. Nat. Commun. 5, 5380. https://doi.org/10.1038/ncomms6380.

Woo, C.-W., Roy, M., Buhle, J.T., Wager, T.D., 2015. Distinct brain systems mediate the effects of nociceptive input and self-regulation on pain. PLoS Biol. 13, e1002036 https://doi.org/10.1371/journal.pbio.1002036.

Woo, C.-W., Schmidt, L., Krishnan, A., Jepma, M., Roy, M., Lindquist, M.A., Atlas, L.Y., Wager, T.D., 2017. Quantifying cerebral contributions to pain beyond nociception. Nat. Commun. 8, 14211. https://doi.org/10.1038/ncomms14211.

Wright, R.A., Mlynski, C., 2019. Fatigue Determination of Inhibitory Strength and Control: A Babe in a Bath. Motiv Sci. 5, 66–78. https://doi.org/10.1037/mot0000114.